Bioorganic Chemistry 37 (2009) 70–76

Contents lists available at ScienceDirect

Bioorganic Chemistry

journal homepage: www.elsevier.com/locate/bioorg

Absolutely conserved tryptophan in M49 family of peptidases contributes to catalysis and binding of competitive inhibitors

Jasminka Špoljarić [a], Branka Salopek-Sondi [b], Janja Makarević [a], Bojana Vukelić [a], Dejan Agić [c], Šumski Šimaga [a], Nina Jajčanin-Jozić [a], Marija Abramić [a,*]

[a] Division of Organic Chemistry and Biochemistry, Ruđer Bošković Institute, Bijenička cesta 54, P.O. Box 180, HR-10002 Zagreb, Croatia
[b] Division of Molecular Biology, Ruđer Bošković Institute, Bijenička cesta 54, P.O. Box 180, HR-10002 Zagreb, Croatia
[c] Department of Chemistry, Faculty of Agriculture, The Josip Juraj Strossmayer University, Trg Sv. Trojstva 3, P.O. Box 719, HR-31107 Osijek, Croatia

ARTICLE INFO

Article history:
Received 26 October 2008
Available online 20 March 2009

Keywords:
Dipeptidyl peptidase III
Hydroxamate inhibitor
Peptidase family M49
Protein structure-function
Site-directed mutagenesis

ABSTRACT

The role of the unique fully conserved tryptophan in metallopeptidase family M49 (dipeptidyl peptidase III family) was investigated by site-directed mutagenesis on human dipeptidyl peptidase III (DPP III) where Trp300 was subjected to two substitutions (W300F and W300L). The mutant enzymes showed thermal stability equal to the wild-type DPP III. Conservative substitution of the Trp300 with phenylalanine decreased enzyme activity 2–4 fold, but did not significantly change the K_m values for two dipeptidyl 2-naphthylamide substrates. However, the K_m for the W300L mutant was elevated 5-fold and the k_{cat} value was reduced 16-fold with Arg-Arg-2-naphthylamide. Both substitutions had a negative effect on the binding of two competitive inhibitors designed to interact with S1 and S2 subsites.

These results indicate the importance of the aromatic nature of W300 in DPP III ligand binding and catalysis, and contribution of this residue in maintaining the functional integrity of this enzyme's S2 subsite.

1. Introduction

Metallopeptidase family M49 (dipeptidyl peptidase III family) has been recognized recently, based on the similarity in amino acid sequences of its members and the structural motif HEXXXH, important for zinc ligation and catalytic activity. Until now, dipeptidyl peptidase III (DPP III; EC 3.4.14.4; formerly known as dipeptidyl aminopeptidase III) was purified and biochemically characterized from several human and animal tissues, and lower eukaryotes [1]. The cDNA for human, rat and fruit fly DPP III was cloned and their respective amino acid sequences (737, 738 and 786 amino acids long) were deduced [1–3]. DPP III in vitro hydrolyzes distinctive synthetic substrate Arg-Arg-2-naphthylamide (Arg_2-2NA) [4] and a number of biologically active peptides, cleaving dipeptides sequentially from their N-termini. Besides its contribution in normal intracellular protein catabolism, the regulatory and pathophysiological role for DPP III was suggested [1]. Human DPP III was recognized by us as a biochemical indicator of endometrial and ovarian malignancies [5,6]. Others indicated the role for DPP III in the endogenous pain-modulatory system, defense against oxidative stress and in cataractogenesis [7–9]. Recently we discovered that DPP III could, in some of its substrates (endomorphin-1 and -2, β-casomorphin), act as a post-proline-cleaving enzyme, contrary to the previous notion that this amino acid imposes restrictions on the hydrolysis of peptide bonds catalyzed by the DPP III type of enzyme [10].

Mutational analysis of rat DPP III identified that two histidines of the characteristic hexapeptide HELLGH motif (residues 450–455) and Glu508 are involved in coordination of the active-site zinc, and that the glutamic acid residue at position 451 is crucial for DPP III catalytic activity [11]. A functional role for Tyr318 was demonstrated at the active site of human DPP III by using the same approach [12].

Most recently, the crystal structure of the yeast DPP III (ligand-free) was resolved representing a prototype for the whole DPP III (M49) family [13]. It is a novel protein fold with two domains forming a cleft containing the active site with catalytic metal ion. However, in the absence of experimental structures of DPP III-substrate (inhibitor) complexes, the ligand binding is still speculative, i.e. the structural basis of DPP III broad substrate specificity is largely unknown. Previous study on human DPP III, based on the determination of affinity constants of this enzyme for a variety of peptides suggested hydrophobic S1' subsite [14].

To reveal yet unknown constituents of (human) DPP III substrate binding site, as a prerequisite, we performed a multiple alignment of all the DPP III (M49 peptidase) sequences (from more than 50 species) present in the databases and have revealed that only one Trp (in position 300 in mammalian amino acid sequences) is absolutely conserved (Fig. 1 illustrates alignment of DPP III sequences from 11 different species).

* Corresponding author. Fax: +385 1 4680 195.
E-mail address: abramic@irb.hr (M. Abramić).

0045-2068/$ - see front matter © 2009 Elsevier Inc. All rights reserved.
doi:10.1016/j.bioorg.2009.03.002

Assuming that evolutionary constraint implies the functional role for this tryptophan, we considered Trp300 to be good candidate for a residue contributing to a hydrophobic pocket of human DPP III. In this study, we substituted it by site-directed mutagenesis, and examined the effects of its replacement on enzyme's catalytic properties and the binding of hydroxamate inhibitors.

2. Materials and methods

2.1. Construction of the expression vector of human DPP III

Clone IRALp962E0242Q2, containing the full length cDNA encoding human DPP III from tissue of renal cell adenocarcinoma, was purchased from the RZPD German Resource Center for Genome Research (Berlin, Germany). A PCR amplification of the DPP III gene of 2.214 kb was achieved using a forward (5′-gcagcagctagcatggcggacacccagtacatcc-3′) and a reverse primers (5′-agggccgtcgacagccttggtctgatggaattgg-3′), carrying *Nhe*I and *Sal*I restriction sites, respectively. PCR was performed according to standard procedures using recombinant Taq DNA polymerase (Takara Bio inc., Japan) and the following program: initial denaturation at 94 °C for 5 min, 30 cycles at 94 °C for 30 s, 60 °C for 60 s, 72 °C for 5 min, and final extension at 72 °C for 7 min. Following restriction digestion of the PCR product and pET21b plasmid with *Nhe*I and *Sal*I restriction enzymes (Invitrogen, USA), ligation was performed by T4 DNA ligase (Invitrogen, USA) for 2 h at room temperature, and *Escherichia coli* XL-10 Gold cells (Stratagene, USA) were transformed. Colonies, grown over night, were subjected to colony PCR for screening, and that positive for DPP III fragment were subjected to plasmid isolation by using GenElute Plasmid Miniprep Kit (Sigma, Germany). Since this construct contained three codons (for methionine, alanine and serine) belonging to pET21b plasmid sequence before the first AUG codon of the cloned DPP III gene, deletion of these codons was performed by using QuickChange II XL Site-Directed Mutagenesis kit (Stratagene, USA) and the following set of complementary primers: 5′-gaaggagatatacatatggcggacacccagtacatcc-3′, and 5′-ggatgtactgggtgtccgccatatgtatatctccttc-3′. It resulted in the final construct which was used for further mutagenesis and protein expressions.

2.2. Site-directed mutagenesis and sequencing

Point mutations of the DPP III gene: W300F, and W300L were carried out with the QuickChange II XL Site-Directed Mutagenesis kit (Stratagene, USA) by using the primers listed in Table 1. The sequencing of complete DPP III gene, as well as confirmation of each mutant, were obtained with automated sequence analyzer "ABI PRISM® 3100-Avant Genetic Analyzer" (Applied Biosystems, USA) using ABI PRISM BigDye Terminator v3.1 Ready Reaction Cycle Sequencing Kit, commercial T7 forward and T7 reverse primers, as well as the following internal DPP III primers: DPPIII271F, 5′-gcgttcctggtctatgccgcggg-3′; DPPIII521F, 5′-ggaattgtaccatggaagatgcc-3′; DPPIII521R, 5′-ggcatcttccatggtacaattcc-3′; DPPIII1261F, 5′-cgggagaagcttacctttctggagg-3′; DPPIII1614R, 5′-ccatgttgagccagttcacgtagatc-3′. All primers were custom synthesized by Invitrogen (USA).

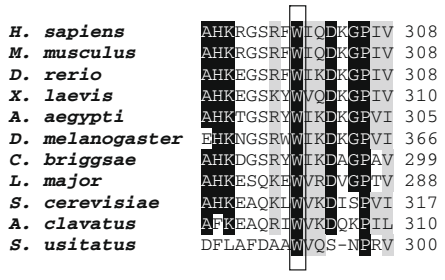

Fig. 1. Conserved Trp in family M49. Multiple sequence alignment of a selection of significantly similar peptidases of DPP III family (peptidase family M49) was obtained using CLUSTAL X v.1.83 [25]. Final presentation shows partial alignment diagram of sequences: *Homo sapiens* (Q9NY33), *Mus musculus* (Q99KK7), *Danio rerio* (Q6DI20), *Xenopus laevis* (Q6PA12), *Aedes aegypti* (Q17GV2), *Drosophila melanogaster* (Q9VHR8), *Caenorhabditis briggsae* (A8XGF7), *Leishmania major* (Q4QJA6), *Saccharomyces cerevisiae* (Q08225), *Aspergillus clavatus* (A1CGS6), and *Solibacter usitatus* (Q02C27). Residues printed in white on black are those identical in at least 8 out 11 aligned proteins, whereas similar amino acid residues are shadowed gray. Fully conserved Trp is framed.

2.3. Heterologous expressions of wild-type and mutants of DPP III protein

For heterologous expressions, a proper construct (wild-type or a certain mutant) was transformed into *E. coli* strain BL21(DE3)RIL$^+$. Several colonies were inoculated into 5 ml of Luria broth (LB) supplemented with ampicillin (100 μg/ml) and grown over night at 37 °C. The following day 5 ml of the o/n cell culture were added into 0.5 L of fresh LB medium containing ampicillin and grown until the A_{600} reached the values of 0.6–0.8. Protein expression was then induced by addition of isopropyl-β-D-1-thiogalactopyranoside (IPTG) to 0.5 mM and the cells were grown for additional 3 h at 23 °C. Bacterial cells were then pelleted by centrifugation at 5000 g, at 4 °C for 20 min, and stored at −20 °C until lysis for protein analysis and purification.

2.4. Purification of recombinant human DPP III

E. coli pellet, containing recombinant human DPP III protein, was suspended in 10 mM Tris–HCl (pH 8.0; 100 μg lysozyme/ml), with 1 mM EDTA, and incubated on ice for 10 min. Following sonication, and incubation with DNase I (Sigma), cell lysate was clarified by centrifugation at 16,000 g and 4 °C for 20 min. The supernatant was subjected to gel filtration on Sephacryl S-200, superfine, column (1.5 × 90 cm), in 50 mM Tris–HCl, 0.2 M NaCl, pH 7.4 buffer. After concentration and desalting, active DPP III fractions were further purified by FPLC on Mono Q 5/5 column (Pharmacia) equilibrated in 50 mM Tris–HCl, 1 mM NaCl, pH 7.4 buffer. The column was rinsed with the starting buffer containing 0.1 M NaCl, and then with a linear 0.1–0.5 M NaCl gradient. Fractions with DPP III activity, eluted between 0.19 and 0.21 M salt, were stored in 22% glycerol at −10 °C.

2.5. SDS–PAGE and Western-immunoblot analysis

Protein purity was confirmed by gel electrophoresis under denaturing conditions. SDS–PAGE and Western blotting were carried out as described earlier [15].

2.6. Enzyme activity assay and determination of kinetic parameters

The enzymatic activities of wild-type and mutant DPP III were determined by a standard assay at 37 °C with Arg_2-2NA as a substrate, using the colorimetric method as previously described [15].

Table 1
Primers used for site-directed mutagenesis of human DPP III cDNA.

Mutant	Nucleotide sequence (5′–3′) Primer I	Nucleotide sequence (5′–3′) Primer II
W300F	ctcccgcttcttcatccaggacaaagg	cctttgtcctggatgaagaagcgggag
W300L	ctcccgcttcttgatccaggacaaagg	cctttgtcctggatcaagaagcgggag

Codons for the mutated residues are underlined.

Kinetic parameters for hydrolysis of Arg_2-2NA and Ala_2-2NA were determined at 25 °C and at pH 8.6 and pH 8.0, respectively, in the presence of 50 μM $CoCl_2$ by initial rate measurements, as previously described [15]. The kinetic parameters were calculated using Lineweaver-Burk and Hanes plots, with Arg_2-2NA concentrations from 2.5 to 120 μM, and Ala_2-2NA from 100 to 1000 μM.

Dixon and [*S*]/*v* versus [*S*] plots were used to establish the type of inhibition exhibited by hydroxamate inhibitor at pH 8.0.

Protein concentrations were determined using the protein-dye binding assay [16], with bovine serum albumin as a standard.

2.7. Thermal stability

Thermal stability measurements were performed by incubating the samples (0.03 μM enzyme in 17 mM Tris–HCl buffer, pH 7.5) at each temperature for 15 min. Residual DPP III activity was determined at the end of the incubation by a standard activity assay.

2.8. Synthesis of hydroxamate inhibitors

The synthesis, *via* N-hydroxy succinimide intermediates [17], of the two dipeptide hydroxamate inhibitors, L-tyrosyl-L-phenylalanine hydroxamic acid (**4**) and L-tyrosyl-glycine hydroxamic acid (**7**) is outlined in Scheme 1. The reaction of Boc-Tyr(OBzl)OSu (**1**) with HPheNHOBzl·CF_3COOH and triethylamine in dry tetrahydrofuran afforded the protected derivative **2**. The O-benzyl groups were deprotected by the hydrogenolysis with 10% Pd/C in ethanol (to improve solubility a small amount of dichlormethane was added) [18]. The final compound **4** was obtained by the treatment of compound **3** with trifluoracetic acid [18]. By the same procedure, Tyr-Gly derivative **7** was prepared.

The identity of synthesized inhibitors **4** and **7** was confirmed by ^1H and ^{13}C NMR spectra (recorded at 300 and 75 MHz, respectively, on a Bruker Avance 300 spectrometer) and by high resolution mass spectra (HRMS). Mass spectra in reflectron mode were obtained on an Applied Biosystems MALDI-TOF/TOF mass spectrometer (Foster City, USA).

4: ^1H NMR (DMSO-d_6): δ 10.75 (1 H, s, –NH–O), 9.43 (1 H, s br, –OH), 8.93 (1 H, d, *J* = 8.3, NH_{Phe}), 8.02 (3H, s, $-NH_3^+$), 7.35–7.17 (5 H, m, $CH_{arom,\ Phe}$), 7.04, 6.71 (2 × 2 H, 2d, *J* = 8.4, $CH_{arom,\ Tyr}$), 4.57–4.38, 4.00–3.80 (2 × 1 H, 2 m, 2CH*), 3.08–2.70 (4 H, m, $CH_{2,Phe}$, $CH_{2,Tyr}$); ^{13}C NMR (DMSO-d_6): δ 167.9, 166.8 (C=O), 156.6, 137.2, 130.3, 129.2, 128.3, 126.5, 124.6, 115.3 (C_{arom}, CH_{arom}), 56.0, 53.5 (CH*), 38.1, 36.2 ($CH_{2,Phe}$, $CH_{2,Tyr}$); HRMS calcd. for $C_{18}H_{21}N_3O_4$: 344.1615 $[M + H]^+$, found 344.1625.

7: ^1H NMR (DMSO-d_6): δ 10.59 (1 H, s, –NH–O), 9.43 (1 H, s br, –OH), 8.79 (1 H, t, *J* = 5.4, NH_{Gly}), 8.13 (3H, s, $-NH_3^+$), 7.05, 6.71 (2x2 H, 2d, *J* = 8.3, CH_{arom}), 4.11–3.89 (1 H, m, CH*), 3.75 (1 H, dd, *J* = 5.8, *J* = 15.9, $CH_{A,Gly}$), 3.63 (1 H, dd, *J* = 5.4, *J* = 15.9, CH_BGly), 2.99 (1 H, dd, *J* = 5.5, *J* = 14.0, $CH_{A,Tyr}$), 2.84 (1 H, dd, *J* = 7.7, *J* = 14.0, $CH_{B,Tyr}$); ^{13}C NMR (DMSO-d_6): δ 168.5, 165.0 (C=O), 156.6, 124.8 (C_{arom}), 130.5, 115.4 (CH_{arom}), 53.8 (CH*), 40.0 ($CH_{2,Gly}$), 36.2 ($CH_{2,Tyr}$); HRMS calcd. for $C_{11}H_{15}N_3O_4$: 254.1135 $[M + H]^+$, found 254.1142.

2.9. Fluorescence measurements

All enzyme samples were dialyzed against 50 mM Tris–HCl, pH 7.4, and adjusted for the same protein absorption at 280 nm (0.03) before the measurements. Steady-state fluorescence measurements were performed on Varian Cary Eclipse spectrofluorimeter, at 20 °C, using 1 cm quartz cuvette. The excitation wavelength was set at 295 nm for selective excitation of tryptophan and emission spectra were collected from 300 to 400 nm. The bandwidth for excitation monochromator was 5 nm and for emission 10 nm. Emission spectra were corrected for the background and dilution effect. Analysis of fluorescence data (obtained from at least 3 measurements) was performed using OriginPro7.5 program and adjacent averaging options.

3. Results and discussion

3.1. Generation and purification of wild-type human DPP III and mutant enzymes

Constructs for the wild-type and for mutants were generated and the genes were overexpressed in *E. coli* BL21(DE3)RIL$^+$ as described in the Section 2. Tryptophan at position 300 in human DPP III was replaced by site-directed mutagenesis to phenylalanine or leucine residue. Mutations were confirmed by DNA sequence analysis. The wild-type DPP III and the produced mutated proteins were purified to apparent homogeneity (SDS–PAGE data not shown). The flow of the purification is presented in Table 2. During purification, the two mutant enzymes showed physical properties essentially identical to those of the wild-type DPP III. Western-immunoblot analysis demonstrated that the wild-type and mutant recombinant proteins appeared as bands with identical molecular mass of 82 kDa (Fig. 2).

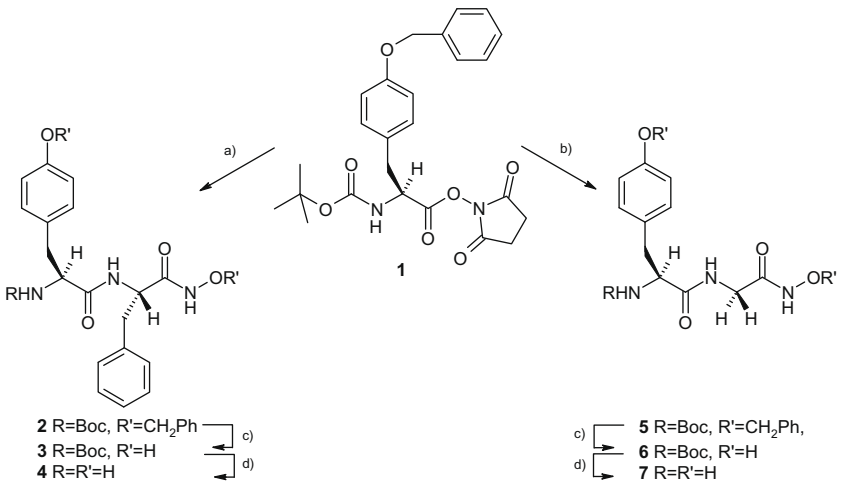

Scheme 1. The synthesis of the hydroxamate inhibitors: (a) H_2N-Phe-NHOBzl·CF_3COOH, TEA, THF; (b) H_2N-Gly-NHOBzl·CF_3COOH, TEA, THF; (c) H_2, 10% Pd/C, EtOH; (d) CF_3COOH.

Table 2
Purification of wild-type and DPP III mutants.

Purification step	Specific activity[a] (U/mg)			Yield (%)		
	Wild-type	W300F	W300L	Wild-type	W300F	W300L
Cell lysate[b]	1.81	1.06	0.05	100	100	100
Gel filtration	25.37	5.38	0.39	71	42	69
FPLC (Mono Q)	45.60	24.90	1.43	28	37	49

[a] Specific activity was determined at 37 °C by a standard assay with Arg_2-2NA, as described in Section 2.
[b] Supernatant 16,000 g.

3.2. Thermal stability

The thermal stability of the mutant and wild-type enzymes is shown in Fig. 3. The curves of the W300F and W300L mutants are coincident with that of the wild-type DPP III: 50% inactivation occurred at approximately 50 °C, while at 55 °C all these enzyme forms were completely inactivated. Identical thermal stability of the wild-type and mutated enzymes suggested that the substitution of Trp300 to Phe or Leu did not affect the overall stability of the protein.

3.3. Substrate specificity towards dipeptidyl 2-naphthylamides

Substrate specificity of mutated enzymes and the wild-type was examined with dipeptidyl 2-naphthylamides. Both mutants and the wild-type preferred Arg_2-2NA (Table 3) which is in agreement with the published data on human erythrocyte DPP III [19]. Ala_2-2NA and Ala-Phe-2NA were hydrolyzed much more slowly (Table 3).

3.4. Kinetic characterization of tryptophanyl mutants

The nomenclature used for the characterization of the individual amino acid residues of a peptide substrate or an inhibitor (P1, P2, P1′) and of the corresponding subsites (S1, S2, S1′) of the enzyme is that of Schechter and Berger [20].

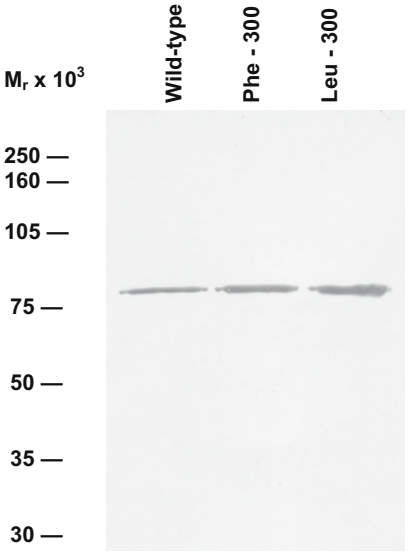

Fig. 2. Western-immunoblot analysis of the purified human DPP III proteins. Samples of wild-type (100 ng/lane) and of recombinant human DPPs III (120 ng of W300F/lane and 150 ng of W300L/lane)) were analyzed by Western blot as described earlier [15].

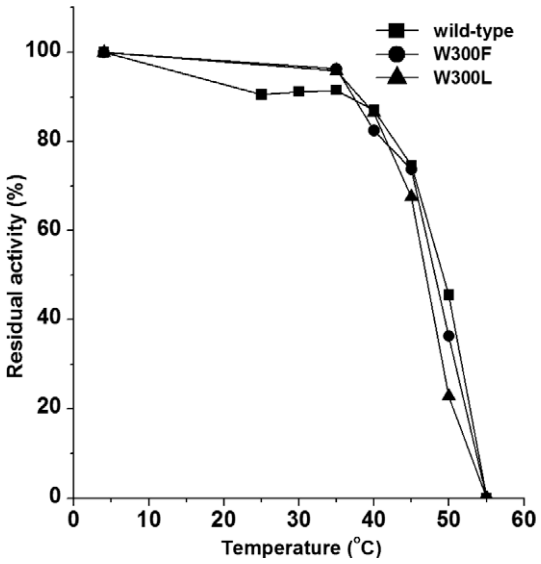

Fig. 3. Effect of temperature on the stability of wild-type and tryptophanyl mutants of human DPP III.

Table 3
Substrate specificity towards dipeptidyl 2-naphthylamides.

Substrate	Relative hydrolysis rate (%)		
	Wild-type DPP III	W300F	W300L
Arg-Arg-2NA	100	100	100
Ala-Ala-2NA	1.64	0.73	2.01
Ala-Phe-2NA	0.25	0.05	1.15
Gly-Phe-2NA	0.02	0.05	0.14

The enzymes were incubated at 37 °C in 50 mM Tris-HCl buffer, pH 8.0 with 50 μM $CoCl_2$ with the substrates at a final concentration of 0.04 mM. (100% = 20.6 μmol or 7.5 μmol or 0.47 μmol of Arg_2-2NA hydrolyzed per min and milligram of the wild-type DPP III, W300F or W300L, respectively).

Catalytic properties of mutants and the wild-type human DPP III were determined using two synthetic substrates which bear identical residue in P1′ position, Arg_2-2NA and Ala_2-2NA. The latter was found to be a much less favorable substrate than Arg_2-2NA for all DPP III forms (Table 4).

The substitution of Trp300 with Phe lowered k_{cat} for the hydrolysis of Arg_2-2NA and Ala_2-2NA 2-fold and 4-fold, respectively, leaving K_m almost unchanged. However, a more dramatic 5-fold increase in K_m and 16-fold decrease in k_{cat} for Arg_2-2NA (78-fold lowered catalytic efficiency, k_{cat}/K_m value) was observed when Trp300 was mutated to Leu (Table 4). Also in the case of a poor substrate (Ala_2-2NA), the decrease in catalytic efficiency of W300L versus the wild-type was more pronounced (22-fold) than that of W300F (5-fold).

Based on the kinetic investigation of hydrolysis of dipeptidyl 2-naphthylamides it is evident that the substitution of evolutionary conserved Trp by a Phe or Leu did not change the preference for these synthetic substrates (overall substrate specificity) (Table 3), but significantly impaired catalytic properties of mutated DPP III (Table 4). More pronounced change of both kinetic parameters, K_m and k_{cat}, observed with W300L indicates the importance of aromatic amino acid residue in that position (300) for catalytic mechanism of DPP III.

The decrease in catalytic efficiency of W300L is comparable with the loss of catalytic power (a 125-fold decrease in k_{cat}/K_m)

Table 4
Kinetic characterization of wild-type and DPP III mutants[a].

	Wild-type	W300F	W300L
Arg-Arg-2NA			
K_m (μM)	11.6 ± 1.4	13.8 ± 0.8	57.0 ± 4.2
k_{cat} (s^{-1})	21.8 ± 2.8	10.7 ± 1.5	1.4 ± 0.0
k_{cat}/K_m ($mM^{-1}\ s^{-1}$)	1879.3	775.4	24.6
Ala-Ala-2NA			
K_m (μM)	299.9 ± 3.4	355.7 ± 46.2	441.1 ± 26.7
k_{cat} (min^{-1})	21.0 ± 0.5	5.1 ± 0.9	1.4 ± 0.2
k_{cat}/K_m ($mM^{-1}\ min^{-1}$)	70.0	14.3	3.2

[a] The kinetic parameters were determined from the initial reaction rates at 25 °C with the Arg_2-2NA concentrations from 2.5 to 120 μM and Ala_2-2NA from 100 to 1000 μM, using a Lineweaver-Burk plot. The enzyme concentrations were: 3.8×10^{-11} M wild-type, 8.8×10^{-11} M W300F and 6.6×10^{-10} M W300L in reaction mixture with Arg_2-2NA, and 2.0×10^{-9} M wild-type, 4.3×10^{-9} M W300F and 1.4×10^{-8}M W300L, respectively, when hydrolysis of Ala_2-2NA was measured. K_m and k_{cat} shown are means ± S.E. for three separate determinations.

in Y318F mutant of human DPP III, shown by us most recently [12]. However, the substitution of Tyr318 did not influence the K_m value and its involvement in transition state stabilization was suggested [12].

3.5. Inhibition with dipeptidyl hydroxamic acids

In order to further characterize the mutated enzymes, their interaction with two dipeptidyl hydroxamic acids, Tyr-Phe-NHOH and Tyr-Gly-NHOH, was investigated. Most recently we have shown strong inhibition of the wild-type human DPP III by Tyr-Phe-NHOH [12]. Therefore, at first, affinity of mutants for this dipeptidyl hydroxamic acid was determined. As shown in Table 5, W300F and W300L were both potently inhibited. The competitive character of this inhibition, illustrated in Fig. 4, was confirmed by *s/v* versus *s* plots (not shown). Interestingly, the mutants' affinity for Tyr-Phe-NHOH was significantly (6-fold of W300F, and 29-fold of W300L, respectively) reduced in comparison to that of the wild-type DPP III (Table 5). More pronounced increase of K_i observed with W300L, compared to W300F, indicates the importance of aromatic amino acid residue in position 300 for inhibitor binding.

To investigate if a hydroxamic acid moiety is sufficient for strong binding to the active site of human DPP III, we changed amino acid in the position P1 (Phe for Gly) in hydroxamate inhibitor. As seen in Table 5, replacement of Phe by Gly in dipeptidyl hydroxamic acid caused dramatic change in inhibitory potency for the wild-type human DPP III and both mutated enzymes. Almost identical increase (70 to 82-fold) in K_i values for Tyr-Gly-NHOH was observed for the wild-type and enzymes with substituted Trp300 compared to the K_i determined for inhibition by Tyr-Phe-NHOH (Table 5).

The inhibitor interaction with DPP III was followed also by fluorimetry. The intrinsic fluorescence properties of the wild-type and tryptophan mutant enzymes were analyzed (Supplemental Fig. 1). Emission spectra were obtained after excitation at 295 nm. The wild-type, W300F and W300L had emission maxima at 333 (332.7 ± 0.6), 337 (336.7 ± 1.2) and 339 (339.0 ± 1.0) nm, respectively. Compared with the wild-type, mutated enzymes W300F and W300L showed a decrease in the fluorescence intensity, measured at a peak maxima, of about 21% and 14%, respectively.

Table 5
Affinity of human DPP III wild-type and mutants for dipeptidyl hydroxamic acids.

	Wild-type, K_i (μM)	W300F, K_i (μM)	W300L, K_i (μM)
Tyr-Phe-NHOH	0.15[a] ± 0.04	0.92 ± 0.12	4.27 ± 1.44
Tyr-Gly-NHOH	10.50 ± 2.10	61.62 ± 1.29	351.62 ± 88.80

[a] K_i of the wild-type human DPP III for Tyr-Phe-NHOH was published recently by us [12]. Presented are means ±S.E. for three separate determinations. K_i values were determined with Arg_2-2NA as substrate at pH 8.0, using Dixon plots.

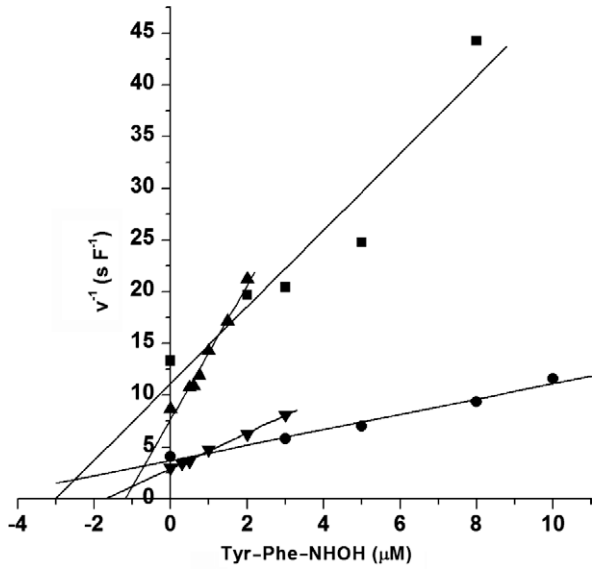

Fig. 4. Inhibition of human DPP III tryptophanyl mutants by Tyr-Phe-NHOH. ● and ■: W300L; ▲ and ▼: W300F. The data are shown as Dixon plots. The K_i corresponds to the negative *X*-axis value of the intersection of the lines obtained at various substrate concentrations: (■, ▲) 5.0 μM; (●, ▼) 20 μM. The initial velocities are expressed in arbitrary units F(fluorescence) s^{-1}.

Addition of inhibitor in saturating concentration resulted in a rapid fluorescence decrease. The steady-state tryptophan fluorescence of human DPP III wild-type was quenched 7.9% by the competitive inhibitor Tyr-Phe-NHOH (Supplemental Fig. 1). The fluorescence of the W300F enzyme was slightly less sensitive to the occupancy of the binding site with competitive inhibitor (7.7% decrease of fluorescence), and that of the W300L mutant showed 5.5% decrease (Supplemental Fig. 1).

Human DPP III is spectroscopically very complex because it has 10 Trp per molecule. Therefore, the interpretation of fluorescence measurements is not unambiguous. Our results indicate that the contribution of Trp300 to the overall protein fluorescence is rather moderate. The finding that W300L showed smaller fluorescence quenching upon inhibitor binding than the wild-type enzyme might indicate the involvement of Trp300. On the other hand, the presence of quenching phenomenon, although in some smaller extent than in the wild-type enzyme, in the W300 mutants could indicate involvement of additional Trp(s) in human DPP III ligand binding. However, evaluation of the contribution of Trp300 to the competitive inhibitor binding using fluorescence measurement could be additionally hindered by the change (which might be increase or decrease) in fluorescence of some other Trp (there are nine Trp residues in addition to Trp300 in human DPP III molecule), which may be remote from the active-site cleft but could also reflect possible conformational changes induced by ligand binding. For instance, Cheung and Mas have shown for 3-phosphoglycerate kinase, another enzyme with an active-site cleft between the two domains, by using fluorescence measurements of single tryptophan probes which were not in direct contact with substrates, that binding of substrates to one domain can also induce spectral perturbation of the probes in the opposite domain [21]. For the yeast DPP III, a TLS (Translation/Libration/Screw) – analysis indicated an opening and closing motion of the substrate binding cleft, i.e. an interdomain movement [13]. A high degree of conservation around

the zinc-binding site and the proposed active-site cleft is found among eukaryotic DPP III enzymes [13].

Due to their ability to form bidentate complexes with metal located in the metallopeptidase catalytic site, hydroxamic acid derivatives are among the most potent inhibitors of such enzymes. Particularly peptidyl hydroxamates have potential for developing of affinity probes for metalloproteases [22,23].

We selected a substrate analog Tyr-Phe-NHOH containing a hydroxamic acid moiety as a zinc coordinating ligand and a dipeptide with a free N-terminal amino group for binding to S1 and S2 subsites (Fig. 5). Tyr-Phe-NHOH was shown by Chérot et al. [24] to be selective inhibitor of enkephalin-degrading dipeptidyl aminopeptidase from the membranes of porcine brain, which inhibited this enzyme competitively with a K_i value of 9 nM at pH 7.0. In our previous work we have used this hydroxamate derivative to investigate the role of Tyr318 in the catalysis of human DPP III. The wild-type DPP III and the Phe318 mutant were inhibited by Tyr-Phe-NHOH, with virtually the same K_i value, indicating that this inhibitor binds similarly in the mutated active site, and that Tyr318 is not the constituent of S1 or S2 subsite. In contrast, in the present study the decreased binding of two competitive inhibitors to the Trp300 mutants implies the role of this fully conserved tryptophan residue in substrate (ligand) binding of M49 peptidases.

Furthermore, our results show that, for strong interactions of DPP III with hydroxamate inhibitor, chelating effect of the hydroxamate moiety is not sufficient. Of crucial importance are interactions with substrate binding subsites. Since the difference in affinity of the wild-type DPP III and of tryptophanyl mutants for Tyr-Phe-NHOH and Tyr-Gly-NHOH was almost two orders of magnitude (Table 5), it is evident that P1 residue of the dipeptidyl hydroxamic acid inhibitor strongly influences the binding (to the S1 subsite of the enzyme). As the decrease for binding of Tyr-Gly-NHOH in both mutated enzymes (W300F and W300L) was practically the same as in the wild-type, Trp300 does not seem to contribute to the enzyme's S1 subsite. However, as K_i values of these two inhibitors designed to bind to the S1 and S2 subsites of dipeptidyl aminopeptidase were greatly increased compared to the K_i value of the wild-type DPP III, these results indicate that Trp300 might participate in maintaining the functional integrity of enzyme's S2 subsite (Fig. 5). Fig. 5 depicts the binding of L-Tyr-L-Phe-NHOH in DPP III active site. It is assumed that dipeptide inhibitor interacts with its N-terminal group with a putative negatively charged acceptor group and that the hydroxamate moiety interacts with the zinc of the catalytic site.

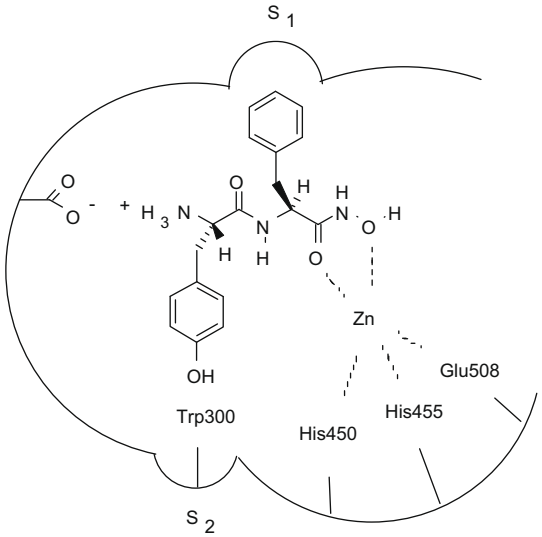

Fig. 5. Schematic representation of the active site of human DPP III binding a competitive inhibitor Tyr-Phe-NHOH.

4. Conclusions

In order to investigate the functional role of the unique evolutionary conserved tryptophan residue in DPP III family of metallopeptidases, recombinant human DPP III (the wild-type and two mutant enzymes, W300F and W300L) was heterologously expressed, purified and kinetically characterized.

In addition, two dipeptidyl hydroxamic acids, Tyr-Phe-NHOH and Tyr-Gly-NHOH, were synthesized and, for the first time, shown to be potent competitive inhibitors of human DPP III.

Obtained kinetic results support the contribution of Trp300 in the ligand (competitive peptide inhibitor) binding and catalysis of human DPP III. Effect of mutations (Trp300 to Phe and Leu) on enzyme's affinity for inhibitors designed to bind to the S1 and S2 subsites indicates that this residue might participate in maintaining the functional integrity of enzyme's S2 subsite.

This investigation provided information on the functional role of Trp300 in human DPP III and on the dipeptidyl hydroxamic acids as potent competitive inhibitors of this metallopeptidase.

Acknowledgments

Support for this study by the Croatian Ministry of Science, Education and Sport (Projects 098-1191344-2938, 098-0982913-2829 and 098-0982904-2912) is gratefully acknowledged. Authors thank Dr. Mario Gabričević for his generous help with fluorescence measurements.

Appendix A. Supplementary material

Supplementary data associated with this article can be found, in the online version, at doi:10.1016/j.bioorg.2009.03.002.

References

[1] J.-M. Chen, A.J. Barrett, in: A.J. Barrett, N.D. Rawlings, J.F. Woessner (Eds.), Handbook of Proteolytic Enzymes, second ed., vol. 1, Elsevier, Amsterdam, 2004, pp. 809–812.
[2] K. Fukasawa, K.M. Fukasawa, M. Kanai, S. Fujii, J. Hirose, M. Harada, Biochem. J. 329 (1998) 275–282.
[3] C. Mazzocco, K.M. Fukasawa, P. Auguste, J. Puiroux, Eur. J. Biochem. 270 (2003) 3074–3082.
[4] S. Ellis, J.M. Nuenke, J. Biol. Chem. 242 (1967) 4623–4629.
[5] Š. Šimaga, D. Babić, M. Osmak, J. Ilić-Forko, Lj. Vitale, D. Miličić, M. Abramić, Eur. J. Cancer 34 (1998) 399–405.
[6] Š. Šimaga, D. Babić, M. Osmak, M. Šprem, M. Abramić, Gynecol. Oncol. 91 (2003) 194–200.
[7] T. Chiba, Y.-H. Li, T. Yamane, O. Ogikubo, M. Fukuoka, R. Arai, S. Takahashi, T. Ohtsuka, I. Ohkubo, N. Matsui, Peptides 24 (2003) 773–778.
[8] Y. Liu, J.T. Kern, J.R. Walker, J.A. Johnson, P.G. Schultz, H. Luesch, Proc. Natl. Acad. Sci. USA 104 (2007) 5205–5210.
[9] H. Zhang, Y. Yamamoto, S. Shumiya, M. Kunimatsu, K. Nishi, I. Ohkubo, K. Kani, Histochem. J. 33 (2001) 511–521.
[10] M. Baršun, N. Jajčanin, B. Vukelić, J. Špoljarić, M. Abramić, Biol. Chem. 388 (2007) 343–348.
[11] K. Fukasawa, K.M. Fukasawa, H. Iwamoto, J. Hirose, M. Harada, Biochemistry 38 (1999) 8299–8303.
[12] B. Salopek-Sondi, B. Vukelić, J. Špoljarić, Š. Šimaga, D. Vujaklija, J. Makarević, N. Jajčanin, M. Abramić, Biol. Chem. 389 (2008) 163–167.
[13] P. Kumar Baral, N. Jajčanin-Jozić, S. Deller, P. Macheroux, M. Abramić, K. Gruber, J. Biol. Chem. 283 (2008) 22316–22324.
[14] M. Abramić, M. Zubanović, Lj. Vitale, Biol. Chem. Hoppe-Seyler 369 (1988) 29–38.
[15] M. Abramić, Š. Šimaga, M. Osmak, L. Čičin-Šain, B. Vukelić, K. Vlahoviček, Lj. Dolovčak, Int. J. Biochem. Cell Biol. 36 (2004) 434–446.
[16] M.M. Bradford, Anal. Biochem. 72 (1976) 248–254.
[17] Methoden Org. Chem. (Houben-Weyl) fourth ed., vol. XV/2, 1974, pp. 149–166.

[18] T. Greene, P.G.M. Wuts, Protecting Groups in Organic Synthesis, John Wiley&Sons Inc., 1991.
[19] M. Abramić, D. Schleuder, Lj. Dolovčak, W. Schröder, K. Strupat, D. Šagi, J. Peter-Katalinić, Lj. Vitale, Biol. Chem. 381 (2000) 1233–1243.
[20] I. Schechter, A. Berger, Biochem. Biophys. Res. Commun. 27 (1967) 157–159.
[21] C.-W. Cheung, M.T. Mas, Protein Sci. 5 (1996) 1144–1149.
[22] E.W.S. Chan, S. Chattopadhaya, R.C. Panicker, X. Huang, S.Q. Yao, J. Am. Chem. Soc. 126 (2004) 14435–14446.
[23] A. Saghatelian, N. Jessani, A. Joseph, M. Humphrey, B.F. Cravatt, Proc. Natl. Acad. Sci. USA 101 (2004) 10000–10005.
[24] P. Chérot, J. Devin, M.-C. Fournié-Zaluski, B.P. Roques, Mol. Pharmacol. 30 (1986) 338–344.
[25] J.D. Thompson, T.J. Gibson, F. Plewniak, F. Jeanmougin, D.G. Higgins, Nucleic Acids Res. 24 (1997) 4876–4882.